

W' and Z' limits for Minimal Walking Technicolor

Jeppe R. Andersen^{♥,*}, Tuomas Hapola^{♥,†} and Francesco Sannino^{♥,‡}
[♥] CP³-Origins & the Danish Institute for Advanced Study DIAS,
 University of Southern Denmark, Campusvej 55, DK-5230 Odense M, Denmark.

We interpret the recent data on non-observation of Z'- and W'-bosons, reported by CMS, within Minimal Walking Technicolor models and use them to constrain the couplings and spectrum of the theory. We provide the reach for both exclusion and possible observation for the LHC with 5 fb⁻¹ at 7 TeV in the centre of mass energy, and 100 fb⁻¹ at 13 TeV.

Preprint: CP³-Origins-2011-16 & DIAS-2011-02

I. INTRODUCTION

Recently the CMS [1] and ATLAS [2] collaborations have reported limits on the masses of possible new spin one resonances, appearing in several Standard Model extensions. These studies are performed using 36-40 pb⁻¹ of data collected during the year 2010. We interpret these results within Minimal Walking Technicolor (MWT) models, where the new spin zero resonances emerge as composite states of the fundamental degrees of freedom.

The electroweak symmetry can naturally break through the formation of a chiral condensate, caused by the existence of new strong dynamics [3, 4]. Theories under the mechanism of dynamical electroweak symmetry breaking (DESB) are called Technicolor. Due to the recent progress [5–18, 18–30] in the understanding of near conformal (walking) dynamics [31, 32] various phenomenologically viable models have been proposed. Primary examples are: the $SU(2)$ gauge theory with two techniflavors in the adjoint representation, known as Minimal Walking Technicolor (MWT) [5]; the $SU(3)$ theory with two flavors in the two-index symmetric representation which is called Next to Minimal Walking Technicolor (NMWT) [5] and the $SU(2)$ theory with two techniflavors in the fundamental representation and one techniflavor in the adjoint representation known as Ultra Minimal Technicolor (UMT) [33]. These gauge theories possess remarkable properties [5, 10–13] and have the smallest effects on precision data when used for Technicolor [5, 13, 34–39]. We have also shown in [40] that the effects of the extensions of the Technicolor models, needed to give masses to the SM fermion, cannot be neglected and lead to models of *ideal walking* of which MWT technicolor models are prime examples. The use of fermions in the fundamental representation of the underlying Technicolor gauge group ensures minimal corrections to the precision data [37–39]. A simple way to achieve this is to gauge, at most, one doublet of techniquarks, as done for the UMT model. More generally these models are known as the partially gauge Technicolor models and were introduced in [10, 13]. The theories underlying the models above are being subject to intensive numerical investigations via lattice simulations [41–65]. The important progress of understanding the phase diagram has led to models where the walking dynamics arises with the minimal matter content serving a natural way to go beyond the Standard Model without fundamental scalars. To motivate better the paradigm of complete absence of fundamental scalars, the authors of [66] have shown that also a successful description of the inflation can be achieved using strong dynamics featuring solely fermionic matter.

II. THE MODEL

In order to respect the triumph of the Standard Model, the extensions have to accommodate the following chiral symmetry breaking pattern:

$$SU(2)_L \times SU(2)_R \rightarrow SU(2)_V. \quad (1)$$

An example of a walking technicolor model embodying just this pattern for the breaking of the global flavor symmetry is the Next to Minimal Walking Technicolor model (NMWT). Any other minimal extension contains the symmetries of NMWT and therefore the common sectors are simultaneously constrained. Here the three technipions produced

*Electronic address: andersen@cp3-origins.net

†Electronic address: hapola@cp3-origins.net

‡Electronic address: sannino@cp3-origins.net

in the breaking of the symmetry are eaten by the W and Z bosons. The low energy spectrum of the theory is described by the spin one vector and axial-vector iso-triplets $V^{\pm,0}$, $A^{\pm,0}$ and the lightest iso-singlet scalar state H . The scalar state can be naturally as light as the SM Higgs [6, 10, 13, 14, 67–69].

The effective Lagrangian [87], given in the Appendix, contains the following set of parameters:

- g and g' , the $SU(2)_L \times U(1)_Y$ gauge couplings;
- μ and λ , the parameters of the scalar potential;
- \tilde{g} , the strength of the spin one resonances interaction;
- m^2 , the $SU(2)_L \times SU(2)_R$ invariant vector-axial mass squared;
- r_2, r_3, s , the couplings between the Higgs and the vector states;

It is convenient to express three of the parameters in terms of G_F , M_Z and α , fixed by the experiments. The parameters r_2 , r_3 and m can be written in terms of the bare axial and vector masses M_A , M_V as follows:

$$m^2 = (M_A^2 + M_V^2 - \tilde{g}^2 v^2 s) / 2, \quad (2)$$

$$r_2 = 2(M_A^2 - M_V^2) / \tilde{g}^2 v^2, \quad (3)$$

$$r_3 = 4M_A^2 \left(1 \pm \sqrt{1 - \tilde{g}^2 S / 8\pi} \right) / \tilde{g}^2 v^2. \quad (4)$$

S is the S-parameter obtained using the zeroth Weinberg Sum Rule (0th WSR). The effective Lagrangian and the features of the theory were first introduced in [34, 70] and efficiently summarized in [79]. Furthermore, M_V and S can be related using the 1st WSR and S is set to 0.3, naively estimated from the underlying Technicolor theory [34, 70]. Thus we are left with the M_A , \tilde{g} , M_H and s as parameters we can vary at the effective Lagrangian level. First principle lattice simulations should be able to determine these parameters in the near future. The walking dynamics nature is associated to the modification of the second WSR according to the discovery made in [71]. The following caveats apply when matching the low energy effective theory to the underlying gauge theory using the modified WSRs [71] as clearly stated in the original paper: One assumes the narrow width approximation; the spectrum is approximated at very low energies by a few resonances while the walking dynamics is modeled using dynamical mass for the technifermions respecting the Schwinger-Dyson scaling behavior.

The new vector and axial-vector states mix with the SM gauge eigenstates yielding the ordinary SM bosons and two triplets of heavy mesons, $R_1^{\pm,0}$ and $R_2^{\pm,0}$, as mass eigenstates. The couplings of the heavy mesons to the SM particles are induced by the mixing. Momentous for this study is how the heavy vectors couple to the fermions. In the region of parameter space where R_1 is mainly an axial-vector and R_2 mainly a vector state, the dependence of the couplings to the SM fermions as a function of \tilde{g} is very roughly

$$g_{R_{1,2}f\bar{f}} \sim \frac{g^2}{\tilde{g}} \quad (5)$$

where g is the electroweak gauge coupling. The full coupling constant is also a function of M_A , but this dependence is very weak.

III. SLICING THE PARAMETER SPACE

To constrain the parameter space of the model we use the recent CMS results [1], which report limits for a W' boson decaying to a muon and a neutrino at $\sqrt{s} = 7$ TeV in the mass range 600 - 2000 GeV for the resonance. ATLAS results are comparable, but the CMS limits are slightly more stringent in the lower mass region, as shown in figure 5 of [2]. Also, the existing data for the dilepton final state can be used to perform this analysis, but currently the limits are weaker than for the lepton plus missing energy final state.

The relevant calculations are performed using MadGraph [80], using the CTEQ6L parton distribution functions [81], and the implementation for the NMWT model [82]. [1] reports experimental limits for the muon channel together with a combined analysis with the electron channel [83]. Slightly different cuts are used for the electron and muon channel. We simplify the analysis slightly, using the most limiting combination of cuts for the theoretical predictions (this leads to insignificant differences). Because of the missing energy in the final state, the invariant mass of the resonance cannot be reconstructed, and the following transverse mass variable is utilized

$$M_T = \sqrt{2 \cdot p_T E_T^{\text{miss}} \cdot (1 - \cos \Delta\phi_{\mu,\nu})}. \quad (6)$$

When considering only two-to-two processes with zero mass final state particles, the angle between the lepton and neutrino is fixed and this definition of the transverse mass reduces to $M_T = 2 \cdot p_T$. In the experimental analysis, the cut on the transverse mass is adjusted in bins of the mass of the sought after resonance. The minimum transverse mass cuts and the physical masses of the vector mesons for three different values of \tilde{g} are given in Table I. The decay widths of the vector mesons are given in Table II. In addition to the transverse mass cut, the lepton acceptance $|\eta| < 2.1$ is used. The resulting cross section is then compared with the limits reported in the experimental analyses.

Exploring the signal from the process $pp \rightarrow R_{1,2} \rightarrow l\nu$ we are able to limit the possible values for the parameters M_A and \tilde{g} . The theoretical limits as well as the limits from the Tevatron are described in [84]. The M_A, \tilde{g} plane of the parameter space is presented in Fig. 1 for $M_H = 200\text{GeV}$ and $s = 0$.

The uniformly shaded region on the left is excluded by the CDF searches of the resonance in the the $p\bar{p} \rightarrow e^+e^-$ process. The striped region in the lower left corner is excluded by the measurements of the electroweak W and Y parameters [85] adapted for models of MWT in [35]. Avoiding imaginary decay constants for the vector and axial-vector sets an upper bound for the \tilde{g} , i.e. excludes the uniformly shaded in the upper part of the figure. The near conformal (walking) dynamics modifies the WRS's, compared to a running case like QCD, as explained above [71]. Imposing these modified sum rules excludes the lower right corner of the parameter space. The CDF exclusion limit is sensitive, indirectly, to the mass of the composite Higgs and the coupling s via properties of the new heavy spin one states. However, the edge of the excluded area varies only very weakly as a function of s and M_H . The CMS search imposes a 95 % CL exclusion bound described with the thick solid (red) line. The thick dashed and dotted lines (blue) are three and five sigma exclusion limits for 7 TeV and 5fb^{-1} . The thin dotted and dashed lines describe the reach of the LHC with 100fb^{-1} at 13 TeV. The three and five sigma exclusion limits are calculated using poisson distribution, following [86]. Due to the effective description, we have not employed the K -factors when calculating the exclusion limits. In Table III we report the explicit values of the signal cross section for given points in the parameter space.

Comparing the three sets of lines for the LHC, the increase in the horizontal direction follows roughly the increase in luminosity. The small role of the center of mass energy can be understood by exploring the behavior of the cross section as a function of the center of mass energy and comparing it with the scaling with \tilde{g} , obtained from equation (5). The Tevatron exclusion line behaves completely differently compared to the lines calculated for the LHC. This follows from the two distinct feature between the machines: In the relevant kinematic, the pdf's are highly gluon dominated at the LHC energies, and the LHC is a proton-proton collider, which further suppresses the portion of the anti-quarks inside the colliding protons compared to the Tevatron.

IV. CONCLUSIONS

We have interpreted experimental bounds from the LHC on new resonances in the e, ν_e and μ, ν_μ -channel within the sector common to all the Minimal Walking Technicolor models. We demonstrated that the data from the LHC are already excluding new regions of the parameter space of strongly coupled extensions of the SM. However much of the parameter space is still allowed, and will be probed by the data arriving in the near future.

TABLE I: Minimum M_T values for different values of the M_A . The last six columns give the physical masses of the $M_{R_{1,2}}$ as a function of M_A , for three different values of the \tilde{g} .

M_A (GeV)	M_T (GeV)	$\tilde{g} = 2$		$\tilde{g} = 4$		$\tilde{g} = 6$	
		M_{R_1} (GeV)	M_{R_2} (GeV)	M_{R_1} (GeV)	M_{R_2} (GeV)	M_{R_1} (GeV)	M_{R_2} (GeV)
600	400	612	704	603	887	601	1142
700	500	714	794	704	945	701	1174
800	500	814	888	804	1008	801	1210
900	500	913	983	905	1075	902	1250
1000	530	1012	1081	1005	1145	1002	1293
1100	590	1111	1180	1106	1218	1102	1339
1200	650	1209	1280	1206	1294	1202	1387
1300	675	1307	1382	1306	1371	1302	1438
1400	675	1404	1484	1406	1450	1402	1491
1500	680	1502	1586	1505	1532	1502	1546
2000	690	1991	2102	1940	2013	1842	2003

Appendix A: Effective Lagrangian

The composite spin-1 and spin-0 states and their interaction with the SM fields are described via the following effective Lagrangian we developed in [34, 70]:

$$\begin{aligned}
 \mathcal{L}_{\text{boson}} = & -\frac{1}{2}\text{Tr}[\widetilde{W}_{\mu\nu}\widetilde{W}^{\mu\nu}] - \frac{1}{4}\widetilde{B}_{\mu\nu}\widetilde{B}^{\mu\nu} - \frac{1}{2}\text{Tr}[F_{L\mu\nu}F_L^{\mu\nu} + F_{R\mu\nu}F_R^{\mu\nu}] \\
 & + m^2 \text{Tr}[C_{L\mu}^2 + C_{R\mu}^2] + \frac{1}{2}\text{Tr}[D_\mu M D^\mu M^\dagger] - \tilde{g}^2 r_2 \text{Tr}[C_{L\mu} M C_{R\mu}^\dagger M^\dagger] \\
 & - \frac{i\tilde{g}r_3}{4}\text{Tr}[C_{L\mu}(M D^\mu M^\dagger - D^\mu M M^\dagger) + C_{R\mu}(M^\dagger D^\mu M - D^\mu M^\dagger M)] \\
 & + \frac{\tilde{g}^2 s}{4}\text{Tr}[C_{L\mu}^2 + C_{R\mu}^2]\text{Tr}[M M^\dagger] + \frac{\mu^2}{2}\text{Tr}[M M^\dagger] - \frac{\lambda}{4}\text{Tr}[M M^\dagger]^2
 \end{aligned} \tag{A1}$$

where $\widetilde{W}_{\mu\nu}$ and $\widetilde{B}_{\mu\nu}$ are the ordinary electroweak field strength tensors, $F_{L/R\mu\nu}$ are the field strength tensors associated to the vector meson fields $A_{L/R\mu}$ [88], and the $C_{L\mu}$ and $C_{R\mu}$ fields are

$$C_{L\mu} \equiv A_{L\mu} - \frac{g}{\tilde{g}}\widetilde{W}_\mu, \quad C_{R\mu} \equiv A_{R\mu} - \frac{g'}{\tilde{g}}\widetilde{B}_\mu. \tag{A2}$$

The 2×2 matrix M is

$$M = \frac{1}{\sqrt{2}}[v + H + 2i\pi^a T^a], \quad a = 1, 2, 3 \tag{A3}$$

where π^a are the Goldstone bosons produced in the chiral symmetry breaking, $v = \mu/\sqrt{\lambda}$ is the corresponding VEV, H is the composite Higgs, and $T^a = \sigma^a/2$, where σ^a are the Pauli matrices. The covariant derivative is

$$D_\mu M = \partial_\mu M - i g \widetilde{W}_\mu^a T^a M + i g' M \widetilde{B}_\mu T^3. \tag{A4}$$

When M acquires its VEV, the Lagrangian of Eq. (A1) contains mixing matrices for the spin one fields.

-
- [1] S. Chatrchyan *et al.* [CMS Collaboration], arXiv:1103.0030 [hep-ex].
 - [2] G. Aad *et al.* [ATLAS Collaboration], arXiv:1103.1391 [hep-ex].
 - [3] S. Weinberg, *Phys. Rev. D* **19**, 1277 (1979).
 - [4] L. Susskind, *Phys. Rev. D* **20**, 2619 (1979).

TABLE II: Spin one widths for different values of M_A and \tilde{g} . Note that the increase in the widths for certain ranges of these couplings is due to the opening of new channels as explained in [79]

M_A (GeV)	$\tilde{g} = 2$		$\tilde{g} = 4$		$\tilde{g} = 6$	
	Γ_{R_1} (GeV)	Γ_{R_2} (GeV)	Γ_{R_1} (GeV)	Γ_{R_2} (GeV)	Γ_{R_1} (GeV)	Γ_{R_2} (GeV)
600	0.678	1.89	0.467	57.0	1.88	258
700	0.675	2.24	0.754	36.7	2.96	187
800	0.669	2.71	1.20	23.0	4.45	133
900	0.699	3.25	1.86	14.2	6.50	93.1
1000	0.809	3.84	2.83	9.23	9.27	64.5
1100	1.04	4.50	4.21	7.27	12.9	45.8
1200	1.44	5.25	6.11	7.83	17.7	35.6
1300	2.04	6.14	8.69	10.3	23.9	32.4
1400	2.89	7.22	12.1	13.4	31.7	35.1
1500	4.02	8.55	16.6	17.4	41.5	41.9
2000	16.2	21.9	57.1	61.6	100	138

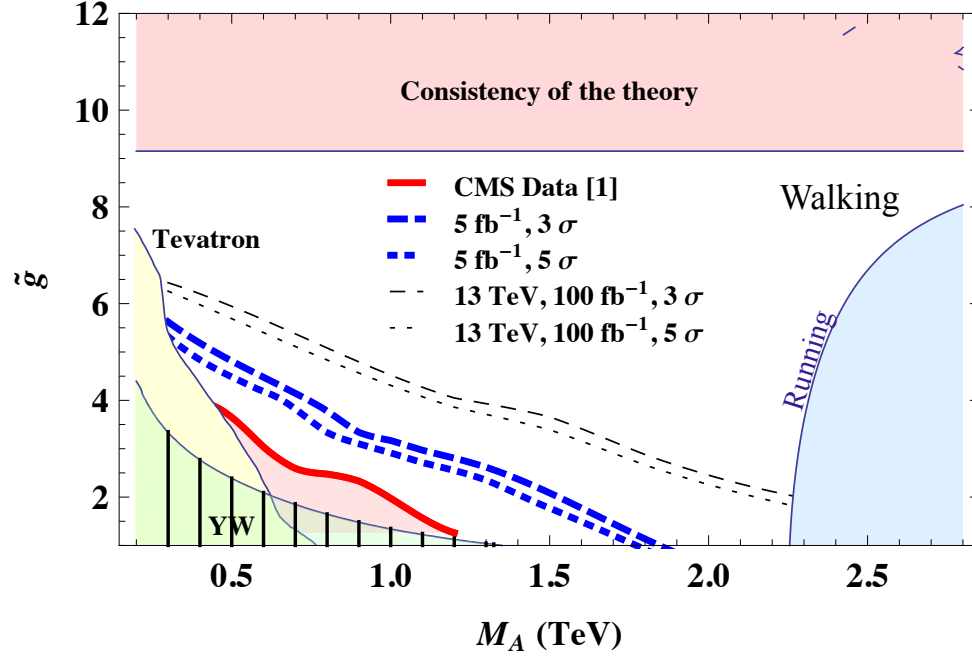


FIG. 1: Bounds in the (M_A, \tilde{g}) plane of the NMWT parameter space: (i) CDF direct searches of the neutral spin one resonance excludes the uniformly shaded area in the left, with $M_H = 200$ GeV and $s = 0$. (ii) The 95 % confidence level measurement of the electroweak precision parameters W and Y excludes the striped area in the left corner. (iii) Imposing the modified WRS's excludes the uniformly shaded area in the right corner. (iv) The horizontal stripe is excluded imposing reality of the axial and axial-vector decay constants. (v) The area below the thick uniform line is excluded by the CMS data [1]. (vi) Dashed and dotted lines are expected exclusions using different values of the integrated luminosity and center of mass energy.

TABLE III: Signal cross sections for given points in the parameter space.

7 TeV		σ (fb)					13 TeV		σ (fb)				
M_A	\tilde{g}	2	2.5	3	3.5	4	M_A	\tilde{g}	3	4	5	6	7
600 (GeV)		-	123	70	39	19	600 (GeV)		-	-	9.4	1.4	0.17
800		100	50	17	7.0	3.0	1500		3.4	0.50	0.10	0.027	0.0085
1000		37	17	6.6	2.1	0.75	2100		0.20	0.033	0.0089	-	-

[5] F. Sannino and K. Tuominen, Phys. Rev. D **71**, 051901 (2005) [arXiv:hep-ph/0405209].
 [6] D. K. Hong, S. D. H. Hsu and F. Sannino, Phys. Lett. B **597**, 89 (2004) [arXiv:hep-ph/0406200].
 [7] H. Gies and J. Jaeckel, Eur. Phys. J. C **46**, 433 (2006) [arXiv:hep-ph/0507171].
 [8] J. Braun and H. Gies, Phys. Lett. B **645**, 53 (2007) [arXiv:hep-ph/0512085].
 [9] J. Braun and H. Gies, JHEP **0606**, 024 (2006) [arXiv:hep-ph/0602226].
 [10] D. D. Dietrich and F. Sannino, Phys. Rev. D **75**, 085018 (2007) [arXiv:hep-ph/0611341].
 [11] T. A. Rytov and F. Sannino, Phys. Rev. D **76**, 105004 (2007) [arXiv:0707.3166 [hep-th]].
 [12] T. A. Rytov and F. Sannino, Phys. Rev. D **78**, 065001 (2008) [arXiv:0711.3745 [hep-th]].
 [13] D. D. Dietrich, F. Sannino and K. Tuominen, Phys. Rev. D **72**, 055001 (2005) [arXiv:hep-ph/0505059].
 [14] F. Sannino, arXiv:0804.0182 [hep-ph]; *idem* Acta Phys. Polon. **B40**, 3533-3743 (2009). [arXiv:0911.0931 [hep-ph]].
 [15] J. Braun and H. Gies, JHEP **1005**, 060 (2010) [arXiv:0912.4168 [hep-ph]].
 [16] O. Antipin and K. Tuominen, Phys. Rev. D **81**, 076011 (2010) [arXiv:0909.4879 [hep-ph]].
 [17] M. Jarvinen and F. Sannino, JHEP **1005**, 041 (2010) [arXiv:0911.2462 [hep-ph]].

- [18] M. Mojaza, C. Pica and F. Sannino, Phys. Rev. D **82**, 116009 (2010) [arXiv:1010.4798 [hep-ph]].
- [19] J. Braun, A. Eichhorn, H. Gies and J. M. Pawłowski, Eur. Phys. J. C **70**, 689 (2010) [arXiv:1007.2619 [hep-ph]].
- [20] J. Alanen, K. Kajantie and K. Tuominen, Phys. Rev. D **82**, 055024 (2010) [arXiv:1003.5499 [hep-ph]].
- [21] C. Pica and F. Sannino, arXiv:1011.3832 [hep-ph].
- [22] C. Pica and F. Sannino, Phys. Rev. D **83**, 035013 (2011) [arXiv:1011.5917 [hep-ph]].
- [23] M. T. Frandsen, T. Pickup, M. Teper, Phys. Lett. **B695**, 231-237 (2011). [arXiv:1007.1614 [hep-ph]]
- [24] T. A. Rytto, R. Shrock, Phys. Rev. **D83**, 056011 (2011). [arXiv:1011.4542 [hep-ph]]
- [25] N. Chen, T. A. Rytto, R. Shrock, Phys. Rev. **D82**, 116006 (2010). [arXiv:1010.3736 [hep-ph]].
- [26] T. A. Rytto, R. Shrock, Phys. Rev. **D81**, 116003 (2010). [arXiv:1006.0421 [hep-ph]].
- [27] T. A. Rytto, R. Shrock, Eur. Phys. J. **C71**, 1523 (2011). [arXiv:1005.3844 [hep-ph]].
- [28] M. Mojaza, M. Nardecchia, C. Pica and F. Sannino, Phys. Rev. D **83**, 065022 (2011) [arXiv:1101.1522 [hep-th]].
- [29] J. Braun, C. S. Fischer and H. Gies, arXiv:1012.4279 [hep-ph].
- [30] M. Jarvinen and F. Sannino, JHEP **1102**, 081 (2011) [arXiv:1009.5380 [hep-ph]].
- [31] B. Holdom, Phys. Rev. D **24**, 1441 (1981).
- [32] B. Holdom, Phys. Lett. B **150**, 301 (1985).
- [33] T. A. Rytto and F. Sannino, Phys. Rev. D **78**, 115010 (2008) [arXiv:0809.0713 [hep-ph]].
- [34] R. Foadi, M. T. Frandsen, T. A. Rytto and F. Sannino, Phys. Rev. D **76**, 055005 (2007) [arXiv:0706.1696 [hep-ph]].
- [35] R. Foadi, M. T. Frandsen and F. Sannino, Phys. Rev. D **77**, 097702 (2008) [arXiv:0712.1948 [hep-ph]].
- [36] R. Foadi, M. Jarvinen and F. Sannino, Phys. Rev. D **79**, 035010 (2009) [arXiv:0811.3719 [hep-ph]].
- [37] F. Sannino, Phys. Rev. D **82**, 081701 (2010) [arXiv:1006.0207 [hep-lat]].
- [38] F. Sannino, Phys. Rev. Lett. **105**, 232002 (2010) [arXiv:1007.0254 [hep-ph]].
- [39] S. Di Chiara, C. Pica and F. Sannino, arXiv:1008.1267 [hep-ph], published in Physics Letters B.
- [40] H. S. Fukano and F. Sannino, Phys. Rev. D **82**, 035021 (2010) [arXiv:1005.3340 [hep-ph]].
- [41] S. Catterall and F. Sannino, Phys. Rev. D **76**, 034504 (2007) [arXiv:0705.1664 [hep-lat]].
- [42] L. Del Debbio, M. T. Frandsen, H. Panagopoulos and F. Sannino, JHEP **0806**, 007 (2008) [arXiv:0802.0891 [hep-lat]].
- [43] Y. Shamir, B. Svetitsky and T. DeGrand, Phys. Rev. D **78**, 031502 (2008) [arXiv:0803.1707 [hep-lat]].
- [44] A. Deuzeman, M. P. Lombardo and E. Pallante, Phys. Lett. B **670**, 41 (2008) [arXiv:0804.2905 [hep-lat]].
- [45] L. Del Debbio, A. Patella and C. Pica, Phys. Rev. D **81**, 094503 (2010) [arXiv:0805.2058 [hep-lat]].
- [46] S. Catterall, J. Giedt, F. Sannino and J. Schneible, JHEP **0811**, 009 (2008) [arXiv:0807.0792 [hep-lat]].
- [47] L. Del Debbio, A. Patella and C. Pica, PoS **LATTICE2008**, 064 (2008) [arXiv:0812.0570 [hep-lat]].
- [48] T. DeGrand, Y. Shamir and B. Svetitsky, Phys. Rev. D **79**, 034501 (2009) [arXiv:0812.1427 [hep-lat]].
- [49] A. J. Hietanen, J. Rantaharju, K. Rummukainen and K. Tuominen, JHEP **0905**, 025 (2009) [arXiv:0812.1467 [hep-lat]].
- [50] A. J. Hietanen, K. Rummukainen and K. Tuominen, Phys. Rev. D **80**, 094504 (2009) [arXiv:0904.0864 [hep-lat]].
- [51] A. Deuzeman, M. P. Lombardo and E. Pallante, Phys. Rev. D **82**, 074503 (2010) [arXiv:0904.4662 [hep-ph]].
- [52] A. Hasenfratz, Phys. Rev. D **80**, 034505 (2009) [arXiv:0907.0919 [hep-lat]].
- [53] L. Del Debbio, B. Lucini, A. Patella, C. Pica and A. Rago, Phys. Rev. D **80**, 074507 (2009) [arXiv:0907.3896 [hep-lat]].
- [54] Z. Fodor, K. Holland, J. Kuti, D. Negradi and C. Schroeder, Phys. Lett. B **681**, 353 (2009) [arXiv:0907.4562 [hep-lat]].
- [55] Z. Fodor, K. Holland, J. Kuti, D. Negradi and C. Schroeder, JHEP **0911**, 103 (2009) [arXiv:0908.2466 [hep-lat]].
- [56] T. DeGrand, Phys. Rev. D **80**, 114507 (2009) [arXiv:0910.3072 [hep-lat]].
- [57] S. Catterall, J. Giedt, F. Sannino and J. Schneible, arXiv:0910.4387 [hep-lat].
- [58] F. Bursa, L. Del Debbio, L. Keegan, C. Pica and T. Pickup, Phys. Rev. D **81**, 014505 (2010) [arXiv:0910.4535 [hep-ph]].
- [59] E. Bilgici *et al.*, Phys. Rev. D **80**, 034507 (2009) [arXiv:0902.3768 [hep-lat]].
- [60] J. B. Kogut and D. K. Sinclair, Phys. Rev. D **81**, 114507 (2010) [arXiv:1002.2988 [hep-lat]].
- [61] A. Hasenfratz, Phys. Rev. D **82**, 014506 (2010) [arXiv:1004.1004 [hep-lat]].
- [62] L. Del Debbio, B. Lucini, A. Patella, C. Pica and A. Rago, Phys. Rev. D **82**, 014509 (2010) [arXiv:1004.3197 [hep-lat]].
- [63] L. Del Debbio, B. Lucini, A. Patella, C. Pica and A. Rago, Phys. Rev. D **82**, 014510 (2010) [arXiv:1004.3206 [hep-lat]].
- [64] S. Catterall, L. Del Debbio, J. Giedt and L. Keegan, PoS **LATTICE2010**, 057 (2010) [arXiv:1010.5909 [hep-ph]].
- [65] Z. Fodor, K. Holland, J. Kuti, D. Negradi and C. Schroeder, arXiv:1103.5998 [hep-lat].
- [66] P. Channuie, J. J. Joergensen and F. Sannino, arXiv:1102.2898 [hep-ph].
- [67] F. Sannino and J. Schechter, Phys. Rev. D **60**, 056004 (1999) [arXiv:hep-ph/9903359].
- [68] A. Doff, A. A. Natale and P. S. Rodrigues da Silva, Phys. Rev. D **77**, 075012 (2008) [arXiv:0802.1898 [hep-ph]].
- [69] M. Fabbri, M. Piai and L. Vecchi, Phys. Rev. D **78**, 045009 (2008) [arXiv:0804.0124 [hep-ph]].
- [70] T. Appelquist, P. S. Rodrigues da Silva and F. Sannino, Phys. Rev. D **60**, 116007 (1999) [arXiv:hep-ph/9906555].
- [71] T. Appelquist and F. Sannino, Phys. Rev. D **59**, 067702 (1999) [arXiv:hep-ph/9806409].
- [72] R. Casalbuoni, S. De Curtis, D. Dominici, R. Gatto, Phys. Lett. **B155**, 95 (1985).
- [73] R. Casalbuoni, A. Deandrea, S. De Curtis, D. Dominici, R. Gatto, M. Grazzini, Phys. Rev. **D53**, 5201-5221 (1996). [hep-ph/9510431].
- [74] R. Casalbuoni, S. De Curtis, D. Dominici, Phys. Lett. **B403**, 86-92 (1997). [hep-ph/9702357].
- [75] D. Dominici, Riv. Nuovo Cim. **20N11**, 1-64 (1997). [hep-ph/9711385].
- [76] M. Battaglia, S. De Curtis, D. Dominici, JHEP **0212**, 004 (2002). [hep-ph/0210351].
- [77] R. S. Chivukula, E. H. Simmons, S. Matsuzaki, M. Tanabashi, Phys. Rev. **D75**, 075012 (2007). [hep-ph/0702218 [HEP-PH]].
- [78] K. Lane, A. Martin, Phys. Rev. **D80**, 115001 (2009). [arXiv:0907.3737 [hep-ph]].
- [79] J. R. Andersen, O. Antipin, G. Azuelos, L. Del Debbio, E. Del Nobile, S. Di Chiara, T. Hapola, M. Jarvinen *et al.*, Eur. Phys. J. Plus **126**, 81 (2011). [arXiv:1104.1255 [hep-ph]].



- [80] J. Alwall *et al.*, JHEP **0709**, 028 (2007) [arXiv:0706.2334 [hep-ph]].
- [81] J. Pumplin, D. R. Stump, J. Huston, H. L. Lai, P. M. Nadolsky and W. K. Tung, JHEP **0207**, 012 (2002) [arXiv:hep-ph/0201195].
- [82] <http://feynrules.phys.ucl.ac.be/wiki/TechniColor>,
<http://cp3-origins.dk/research/tc-tools>.
- [83] V. Khachatryan *et al.* [CMS Collaboration], Phys. Lett. B **698**, 21 (2011) [arXiv:1012.5945 [hep-ex]].
- [84] A. Belyaev, R. Foadi, M. T. Frandsen, M. Jarvinen, F. Sannino and A. Pukhov, Phys. Rev. D **79**, 035006 (2009) [arXiv:0809.0793 [hep-ph]].
- [85] R. Barbieri, A. Pomarol, R. Rattazzi, A. Strumia, Nucl. Phys. **B703**, 127-146 (2004). [hep-ph/0405040].
- [86] G. Aad *et al.* [The ATLAS Collaboration], arXiv:0901.0512 [hep-ex].
- [87] The custodial technicolor limit [35, 70, 71] for certain values of the effective Lagrangian parameters reproduces the BESS model (D-BESS) [72, 73] for which results are available in the literature [74–76]. Following the initial work of [70, 71] several effective Lagrangians similar to the one used here have been proposed in the literature [77, 78], however the present approach is the most general one since it includes besides spin one also the spin zero state. Furthermore, we also provide a direct link, via modified WSRs, to the underlying gauge dynamics. Although this link must be taken with the grain of salt, it is not present in other more phenomenological approaches.
- [88] In Ref. [34], where the chiral symmetry is SU(4), there is an additional term whose coefficient is labeled r_1 . With an SU(N)×SU(N) chiral symmetry this term is just identical to the s term.